IEEE Access
Multidisciplinary | Rapid Review | Open Access Journal

Received December 6, 2021, accepted December 20, 2021, date of publication December 22, 2021,
date of current version December 30, 2021.

Digital Object Identifier 10.1109/ACCESS.2021.3137670

On Entanglement Assisted Classical Optical Communication With Transmitter Side Optical Phase-Conjugation

IVAN B. DJORDJEVIC, (Fellow, IEEE)
Department of Electrical and Computer Engineering, University of Arizona, Tucson, AZ 85721, USA
e-mail: ivan@email.arizona.edu

This work was supported in part by NSF.

ABSTRACT Entanglement assisted (EA) communication has been advocated by numerous authors as a potential alternative to classical communications, in particular in noisy and low-brightness regime. In this paper, I propose an EA scheme employing the optical phase-conjugation (OPC) on transmitter side. I show that the proposed EA communication system, with the transmitter side OPC, significantly outperforms its classical counterpart in low-brightness and highly noisy regime, while employing a classical coherent detection scheme for two-dimensional demodulation. Moreover, the capacity of the proposed EA scheme is significantly higher than EA repetition-BPSK, homodyne, heterodyne, and Holevo capacities. Finally, the proposed EA scheme outperforms the corresponding EA scheme with OPC placed on a receiver side.

INDEX TERMS Entanglement, entanglement assisted capacity, classical communication, Holevo capacity, Shannon capacity.

I. INTRODUCTION

Quantum information processing (QIP) offers new opportunities for secure communications (such as QKD), high-precision quantum sensing, and quantum computing solving the problems that cannot be solved by the classical computers [1]–[3]. Among others, the entanglement is a unique resource for QIP applications. In particular, the quantum communication (QuCom) is the cornerstone to fully exploit the power of entanglement. QuCom enables distribution of entanglement at distance to interconnect quantum devices to endow quantum advantages in sensing, communication, and information gathering. To illustrate, the preshared entanglement has potentials to: (i) enable communications whose security is guaranteed by the quantum mechanics laws, (ii) beat the classical channel capacity [4]–[7], (iii) beat the standard quantum limit for sensing applications, (iv) enable distributed quantum computing, and (v) enable entanglement assisted distributed sensing [8]. These applications require the distribution of entangled signal-idler photon pairs by either fiber-optics-based quantum links or satellite-to-ground links, with one illustrative example being provided in Fig. 1.

The associate editor coordinating the review of this manuscript and approving it for publication was Filbert Juwono.

Even though the optimum encoding for entanglement assisted (EA) communication has been known for decades [4], the design of an optimum receiver for EA communication is still an open problem. It has been demonstrated in [4] that with the two-mode Gaussian states EA capacity can be achieved. In [5] authors proposed employing sufficient number of sections of feedforward sum-frequency generation (FF-SFG) module in corresponding receiver, based on Reference [10]. This scheme was shown to be suitable for use in detection of target in a highly noisy environment [10]; unfortunately, it does not represent the scheme that can achieve the EA channel capacity. To come as close as possible to the EA channel capacity the authors in [5] applied repetition coding over even 10^6 bosonic modes, while covering C, L, and (portion of) S bands. Low-complexity coherent detectors for EA communication are discussed in author's previous paper [7]; however, the OPC on transmitter side has been implicitly assumed but corresponding implementation has not been provided at all. Moreover, similarly as in [5] the shot noise terms due to vacuum state occurring during the OPC on receiver side have been neglected, which overestimates the performance of EA receivers with OPC on receive side, introduced in [5].

In this paper, we propose to perform the optical phase conjugation (OPC), which is required in EA communication

before the photodetection takes place, on transmitter side where the signal photon is brighter rather than on receiver side in [5] when the signal photon has low-brightness and is affected by noise. Moreover, we show that in this case conventional optical homodyne and heterodyne receivers used in classical optical communications are directly applicable in EA communications. We demonstrate that this approach leads to improvements in bandwidth (spectral) efficiencies compared to the case when the OPC is performed on receiver side. We show that the capacity of the proposed EA scheme is significantly higher than homodyne, heterodyne, and Holevo capacities, while outperforming the capacity of the nonlinear receiver with the receive side OPC. Moreover, since low-brightness assumption is not required on transmitter side, the overall transmission distance can be extended.

The organization of the paper is described briefly as follows. In section II, EA communication networks are introduced for completeness of the presentation. In the same section the EA communication model used in the rest of the paper is introduced as well. In Section III, we describe the OPC-based EA receiver. The proposed EA system with transmitter side OPC is described in Section IV. The corresponding EA receiver suitable for arbitrary 2-D constellation is described too. Some relevant, illustrative numerical results are provided in Section V. Finally, the concluding remarks are provided in Sec. VI.

II. ENTANGLEMENT ASSISTED OPTICAL COMMUNICATION NETWORKS

In EA communication networking, we are interested in constructing an EA communication network in which any two users can communicate at rate higher than classical channel capacity. The key issue in such EA networks is to distribute the entangled states across the network and store them in the quantum memories, which are not widely available. As discussed in [6], to distribute the entangled signal-idler photon pairs either the fiber-based quantum links or satellite-to-ground links can be utilized. In the first scenario, shown in Fig. 1, the entangled signal-photon pairs get distributed by the fiber-optics-based network, and are further stored in corresponding quantum memories. Alice uses her signal photon to transmit the classical data towards the remote destination (Bob) over a noisy and lossy Bosonic quantum channel. On the receive side, Bob detects the transmitted signal with the help of the idler photon.

In the second scenario, not shown in the Figure, the satellites are used to distribute entangled signal-photon pairs. Given that satellite-to-ground links are more tolerable to the atmospheric turbulence effects, compared to ground-to-satellite links (due to the shower-curtain effect), the usage of satellite-to-ground links to distribute entanglement seems to be a favorable scenario.

Each signal-idler pair is a two-mode squeezed vacuum (TMSV) state, generated by the spontaneous parametric down conversion (SPDC), and can be represented in Fock basis as

$$|\psi\rangle_{s,i} = (N_s+1)^{-1/2}\sum_{n=0}^{\infty}[N_s/(N_s+1)]^{n/2}\,|\rangle_s\,|\rangle_i, \quad (1)$$

with the mean photon number being $N_s = \left\langle \hat{a}_s^\dagger \hat{a}_s \right\rangle = \left\langle \hat{a}_i^\dagger \hat{a}_i \right\rangle$, with corresponding signal and idler creation operators denoted by $\hat{a}_s^\dagger$ and $\hat{a}_i^\dagger$, respectively. The phase sensitive signal-idler crosscorrelation, defined as $C_{si} = \langle \hat{a}_s \hat{a}_i \rangle = \sqrt{N_s(N_s+1)}$, is used to specify the signal-idler entanglement. Clearly when $N_s \ll 1$ we have that $C_{si} \approx \sqrt{N_s}$, which is significantly larger than the classical limit N_s. The TMSV state is a pure maximally entangled zero-mean Gaussian state with corresponding Wigner covariance matrix being:

$$\mathbf{\Sigma}_{TMSV} = \begin{bmatrix} (2N_s+1)\,\mathbf{1} & 2\sqrt{N_s(N_s+1)}\mathbf{Z} \\ 2\sqrt{N_s(N_s+1)}\mathbf{Z} & (2N_s+1)\,\mathbf{1} \end{bmatrix}, \quad (2)$$

with $\mathbf{1}$ being the identity matrix and $\mathbf{Z} = \mathrm{diag}(1,-1)$ being the Pauli Z-matrix. The SPDC-based entangled source represents a broadband source with $D = T_m W$ i.i.d. signal-idler mode pairs, where W denotes the phase-matching bandwidth and T_m is an interval of the measurement.

The corresponding model for EA classical communication is provided in Fig. 2, wherein the preshared entanglement is distributed by means of two channels: the signal channel, denoted by Φ_s, and the idler channel, denoted by Φ_i.

When the quantum error correction coding has been properly chosen, the entangled quantum states stored in the quantum memories are protected against the decoherence

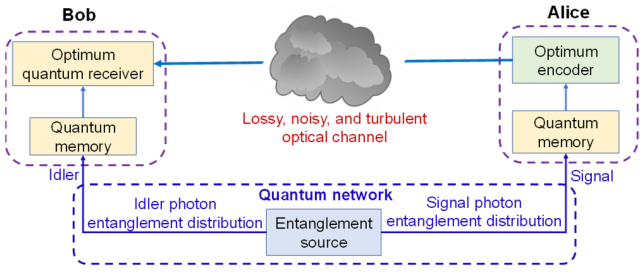

FIGURE 1. The EA classical communication concept enabled by fiber-optics-based distribution of entanglement.

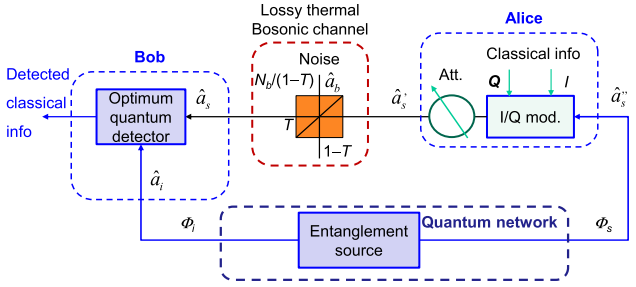

FIGURE 2. The EA communication system model under study. I/Q mod: electro-optical I/Q modulator, Att.: attenuator. The $\hat{a}_b$ denotes the annihilation operator of a thermal (background) mode. The $\hat{a}_s'$ and $\hat{a}_i$ denote annihilation operators of signal and idler photons at the output of entanglement source. After the modulation signal photon creation operator is denoted by $\hat{a}_s^*$. Finally, the signal mode annihilation operator after lossy thermal Bosonic channel is denoted by $\hat{a}_s$.

effects. The main (Alice-to-Bob) channel has been modelled as a single-mode thermal lossy Bosonic channel model as follows:

$$\hat{a}_s = \sqrt{T}\hat{a}_s' + \sqrt{1-T}\hat{a}_b, \tag{3}$$

with T being the transmissivity of the Alice-to-Bob channel, and $\hat{a}_b$ denotes the annihilation operator of a thermal (background) mode with corresponding mean photon number $N_b/(1-T)$.

To improve the bandwidth efficiency of repetition phase encoding scheme over large number of bosonic modes [5], author in [6] proposed to apply the Gaussian modulation (GM) on single photon of the TMSV state, which is illustrated in Fig. 2. Alice performs the GM by generating the I and Q coordinates in electrical domain and using them as the RF inputs to an electro-optical I/Q modulator, wherein Gaussian samples are properly scaled to account for the I/Q modulator insertion loss such that average number of transmitted signal photons per mode is equal to $N_s = \left\langle (\hat{a}_s')^\dagger \hat{a}_s' \right\rangle$. In Reference [6] the following covariance matrix between Alice and Bob is derived:

$$\mathbf{\Sigma}_{AB} = \begin{bmatrix} (2N_s+1)\,\mathbf{1} & 2\sqrt{TN_s(N_s+1)}\mathbf{Z} \\ 2\sqrt{TN_s(N_s+1)}\mathbf{Z} & \left(2N_s'+1\right)\mathbf{1} \end{bmatrix}, \tag{4}$$

where $N_s' = N_s T + N_b$.

III. OPTICAL PHASE CONJUGATION (OPC)-BASED RECEIVER FOR EA COMMUNICATION SYSTEMS

The EA receiver often employs the optical parametric optical amplifier (OPA) as the basic nonlinear building block. Single *OPA-based receiver* is provided in Fig. 3, where the OPA gain is chosen as $G = 1+\varepsilon$, $\varepsilon \ll 1$. The idler output of the OPA is related to the idler annihilation $\hat{a}_i$ and signal creation $\hat{a}_s^\dagger$ operators as follows [12]

$$\hat{A}_i = \sqrt{G}\,\hat{a}_i + \sqrt{G-1}\,\hat{a}_s^\dagger. \tag{5}$$

Under assumption that M-ary PSK is used, the signal mode at the output modulator, denoted as $\hat{a}_s$, is related to the input mode of modulator $\hat{a}_s'$ by $\hat{a}_s = e^{j\phi}\hat{a}_s'$ where ϕ is the phase shift applied by the modulator. The expected value of the photocurrent operator, assuming that photodiode responsivity is $R = 1$ A/W, is related to the photon count average by:

$$\begin{aligned}\left\langle \hat{i} \right\rangle &= \left\langle A_i^\dagger \hat{A}_i \right\rangle \\ &= GN_s + 2\sqrt{G(G-1)}C_{si}\cos\phi + (G-1)\left(N_s'' + 1\right),\end{aligned} \tag{6}$$

where we used the fact that $N_i = N_s$ for TMSV state. Obviously, the photocurrent average is proportional to $\cos\phi$ so that the transmitted phase can be detected, but the detection is affected by two shot noise terms.

Given that OPA receiver is not compatible with the balanced detection, the *optical phase-conjugate* (OPC) receiver can be used instead for that purpose, which is provided in Fig. 4. In OPC-based receiver we employ the OPA to

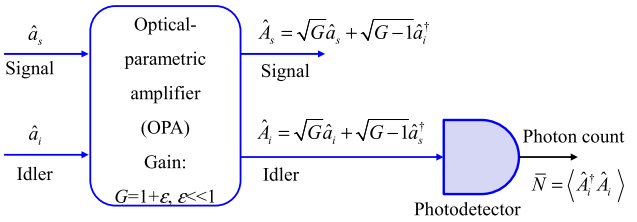

FIGURE 3. The OPA based EA receiver. The photons are detected at the idler output port. Photodetector responsivity is set to $R = 1$ A/W.

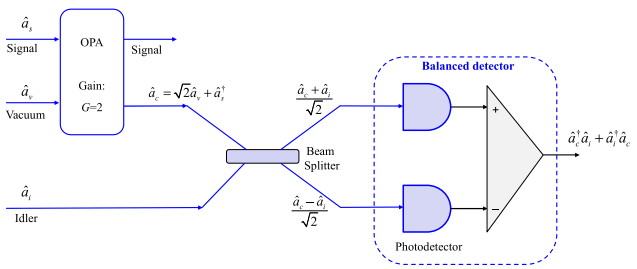

FIGURE 4. The operation principle of the OPC-based EA receiver.

nonlinearly interreact the signal mode $\hat{a}_s$ with the vacuum mode $\hat{a}_v$ to get the following output at the idler port $\hat{a}_c = \sqrt{G}\,\hat{a}_v + \sqrt{G-1}\,\hat{a}_s^\dagger$.

For OPA gain of $G = 2$ the output idler port operator simplifies to $\hat{a}_c = \sqrt{2}\,\hat{a}_v + \hat{a}_s^\dagger$. By mixing the a_c- and idler-modes on a balanced beam splitter (BBS), which is followed by the balanced detection (BD) circuit, the following BD photocurrent operator is obtained:

$$\begin{aligned}\hat{i}_{BD} &= \hat{a}_c^\dagger \hat{a}_i + \hat{a}_i^\dagger \hat{a}_c \\ &= \sqrt{2}\hat{a}_v^\dagger \hat{a}_i + \hat{a}_s \hat{a}_i + \sqrt{2}\hat{a}_i^\dagger \hat{a}_v + \hat{a}_i^\dagger \hat{a}_s^\dagger.\end{aligned} \tag{7}$$

For M-ary PSK because $\hat{a}_s = e^{j\phi}\hat{a}_s'$, we obtain the following expression for the expectation of the BD photocurrent operator:

$$\left\langle \hat{i}_{BD} \right\rangle = e^{j\varphi}\underbrace{\left\langle \hat{a}_s' \hat{a}_i \right\rangle}_{C_{si}} + e^{-j\varphi}\underbrace{\left\langle \hat{a}_i^\dagger \hat{a}_s^\dagger \right\rangle}_{C_{si}} = 2C_{si}\cos\phi, \tag{8}$$

thus canceling the shot noise terms in single-detector case in Eq. (6). In Eq. (8) we assumed that vacuum- and idler-modes are mutually uncorrelated. The BD photocurrent operator variance, by ignoring the terms originating from the vacuum state as it was done in Reference [5], is derived to be:

$$\begin{aligned}Var\left(\hat{i}_{BD}\right) &= \left\langle \hat{i}_{BD}^2 \right\rangle - \left\langle \hat{i}_{BD} \right\rangle^2 \\ &\simeq N_i N_s' + (N_i+1)\left(N_s'+1\right) \\ &\quad + 2C_{si}^2\cos(2\phi) - 4C_{si}^2\cos^2\phi.\end{aligned} \tag{9}$$

Unfortunately, the contributions due to vacuum state cannot be ignored in the weak-brightness regime, which is discussed at the beginning of next section. For binary PSK (BPSK) the expression for variance gets simplified to:

$$Var^{(BPSK)}\left(\hat{i}_{BD}\right) = N_i N_s' + (N_i+1)\left(N_s'+1\right) - 2C_{si}^2. \tag{10}$$

In highly noisy and low-brightness regime, where $N_b \gg 1$ and $N_s \ll 1$, the corresponding expression for variance is simply:

$$Var^{(BPSK)}\left(\hat{i}_{BD}\right) \approx (2N_s + 1)\, N_b, \tag{11}$$

and this expression is identical to that in Reference [5].

IV. PROPOSED ENTANGLEMENT ASSISTED CLASSICAL OPTICAL COMMUNICATION SYSTEM

If we do not ignore the variance terms originating from the vacuum state in the OPC-based EA receiver (Fig. 4), we obtain the following expression for the BD photocurrent operator variance:

$$Var\left(\hat{i}_{BD}\right) = 2\left(N_i + 1\right) + 4N_i + N_i N_s^{''} + \left(N_i + 1\right)\left(N_s^{''} + 1\right) + 2C_{si}^2 \cos\left(2\phi\right) - 4C_{si}^2 \cos^2\phi, \tag{12}$$

which comparted to Eq. (9) contains two extra shot-noise terms.

By moving the OPA to the transmitter side by ensuring that $N_s \gg N_v = 1$, where the signal photon brightness is much higher, the output at the idler output port of the OPA will be just phase-conjugated signal mode, given that contributions originating from vacuum state are negligible in high-brightness regime. This approach allows us to extend transmission distance because now the low-brightness condition becomes $TN_s \ll 1$, and since $N_s \gg 1$ in this scenario the transmission distance can be significantly extended compared to the case when OPC is placed on receiver side. Moreover, the PDC generator and OPA can be integrated on the same chip. Finally, the commercial classical coherent detection schemes are directly applicable to EA detection as described below.

Alternatively, similarly to fiber-optics communications [11], we can use periodically poled $LiNbO_3$ (PPLN) waveguide to realize the phase-conjugation by the difference frequency generation (DFG), and corresponding quantum transmitter is provided in Fig. 5. The first PPLN waveguide is used to generate signal-idler pair through the SPDC process. The signal and idler photons are separated after the first PPLN waveguide. In second PPLN waveguide through the DFG the pump photon ω_p interacts with input signal mode ω_s to get the phase-conjugated signal at $\omega_{s,PC} = \omega_p - \omega_s$. The idler photon is distributed to Bob's receiver by an optical fiber (serving as a quantum memory). This signal mode is modulated by an electro-optical (E/O) modulator, implemented also using the $LiNbO_3$ technology. Therefore, the proposed quantum transmitter is perfectly suited for the integration on the same chip based on the $LiNbO_3$ technology. The E/O modulator can also be swapped with the OPC PPLN waveguide, and in this case the modulation will take place before the phase-conjugation. As an illustration, for the strong pump at $\lambda_p = 780$ nm, through the SPDC an idler photon at $\lambda_i = 1530$ nm and a signal photon at wavelength $\lambda_s = 1591.2$ nm are generated. In the second (OPC) PPLN the signal photon interacts with the pump photon through DFG to get the phase-conjugated (PC) signal photon at

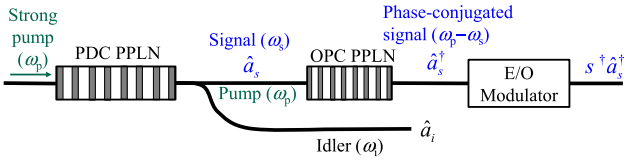

FIGURE 5. The operation principle of integrated quantum transmitter. PDC: parametric down conversion, OPC: optical phase-conjugation, PPLN: periodically poled $LiNbO_3$ waveguide, E/O: electro-optical.

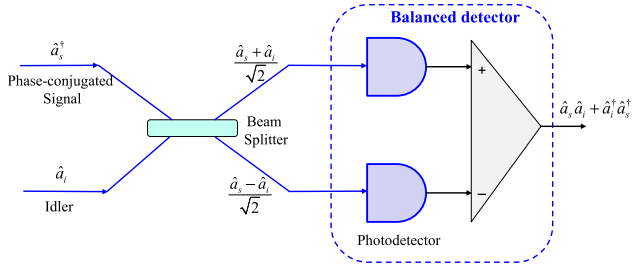

FIGURE 6. The balanced BBS-based homodyne balanced detection receiver used as EA receiver.

$\lambda_{s,PC} = 1/(1/\lambda_p - 1/\lambda_s) = 1530$ nm, at the same wavelength as the idler photon.

By moving the OPC to the transmitter side, we can use balanced detection schemes devised for classical communications in EA detection, with one such scheme provided in Fig. 6, where we mix the phase-conjugated signal and idler modes directly on BBS. The BD photocurrent operator is now simply:

$$\hat{i}_{BD} = \hat{a}_s\hat{a}_i + \hat{a}_i^\dagger\hat{a}_s^\dagger, \tag{13}$$

and the expectation of the BD photocurrent operator, for M-ary PSK with $\hat{a}_s^{'} = e^{j\phi}\hat{a}_s^{''}$ and $T = 1$, is given by:

$$\left\langle\hat{i}_{BD}\right\rangle = e^{j\varphi}\underbrace{\left\langle\hat{a}_s^{''}\hat{a}_i\right\rangle}_{C_{si}} + e^{-j\varphi}\underbrace{\left\langle\hat{a}_i^\dagger\hat{a}_s^{''\dagger}\right\rangle}_{C_{si}} = 2C_{si}\cos\phi, \tag{14}$$

which is identical to that of the OPC receiver [see Eq. (8)]. Clearly, in this classical coherent detection receiver we use the phase-conjugated signal photon at the incoming optical signal port and the idler photon at the local oscillator (LO) laser port. On the other hand, the BD photocurrent operator variance is given by:

$$Var\left(\hat{i}_{BD}\right) = \left\langle\hat{i}_{BD}^2\right\rangle - \left\langle\hat{i}_{BD}\right\rangle^2 = N_i N_s^{''} + \left(N_i + 1\right)\left(N_s^{''} + 1\right) + 2C_{si}^2\cos\left(2\phi\right) - 4C_{si}^2\cos^2\phi, \tag{15}$$

and compared to Eq. (12) it does not have the terms originating from the vacuum state.

Given that this receiver is identical to the coherent detection receiver, in which instead of the LO laser signal the idler mode is used, different coherent detection receivers described in [13] are directly applicable in EA communications. Now we describe an optical hybrid (OH) based EA balanced

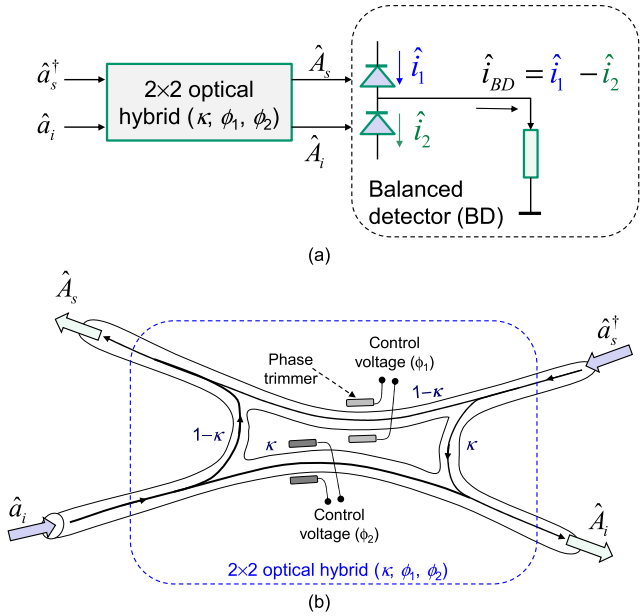

FIGURE 7. The 2 × 2 optical hybrid-based EA balanced detection receiver: (a) EA receiver configuration and (b) integrated optics implementation of 2 × 2 optical hybrid.

detection scheme, shown in Fig. 7, because it is suitable for implementation in integrated optics and as such is compatible with the quantum nanophotonics. In Fig. 7(a), we provide the configuration of 2 × 2 optical hybrid-based BD, while in Fig. 7(b) we provide the corresponding integrated optics implementation of 2 × 2 OH. The OH employs two phase trimmers that are used to introduce corresponding phase shifts φ_1 and φ_2, respectively. The OH contains two input and two output Y-junctions, and the scattering matrix of OH is given by:

$$\boldsymbol{S} = \begin{bmatrix} e^{j\varphi_1}\sqrt{1-\kappa} & \sqrt{1-\kappa} \\ \sqrt{\kappa} & e^{j\varphi_2}\sqrt{\kappa} \end{bmatrix}, \tag{16}$$

where κ is the power splitting ratio of Y-junctions, and this matrix transforms input phase-conjugated signal and idler modes to:

$$\begin{bmatrix} \hat{A}_s \\ \hat{A}_i \end{bmatrix} = \boldsymbol{S} \begin{bmatrix} \hat{a}_s^\dagger \\ \hat{a}_i \end{bmatrix}. \tag{17}$$

By setting the power-splitting ratio as $\kappa = 1/2$, the transformation above simplifies to:

$$\begin{bmatrix} \hat{A}_s \\ \hat{A}_i \end{bmatrix} = \frac{1}{\sqrt{2}} \begin{bmatrix} e^{j\varphi_1} & 1 \\ 1 & e^{j\varphi_2} \end{bmatrix} \begin{bmatrix} \hat{a}_s^\dagger \\ \hat{a}_i \end{bmatrix}. \tag{18}$$

Assuming that arbitrary 2-D constellation is used, the signal mode at the output of I/Q modulator $\hat{a}_s$ is related to the input mode of modulator $\hat{a}_s'$ by $\hat{a}_s = s\hat{a}_s'$, where $s = s_I + js_Q$ is the 2-D signal constellation point. For instance for M-ary PSK, we have that $s = \exp(j\phi)$. Here we assume that E/O modulator is placed before the OPC PPLN waveguide. The idler needs to be properly delayed using a tunable optical fiber so that it matches the propagation delay of the signal photon.

Based on Fig. 7(a), we obtain the following balanced detector photocurrent operator:

$$\hat{i}_{BD} = \frac{1}{2}s\left(e^{-j\varphi_1} - e^{j\varphi_2}\right)a_s' a_i + \frac{1}{2}s^\dagger\left(e^{j\varphi_1} - e^{-j\varphi_2}\right)a_i^\dagger (a_s')^\dagger. \tag{19}$$

The photocurrent operator expectation is given by:

$$\left\langle \hat{i}_{BD} \right\rangle = \frac{1}{2}sC_{si}\left(e^{-j\varphi_1} - e^{j\varphi_2}\right) + \frac{1}{2}s^\dagger\left(e^{j\varphi_1} - e^{-j\varphi_2}\right)C_{si}. \tag{20}$$

By setting $\varphi_1 = 0$ rad and $\varphi_2 = \pi$, we obtain the BD photocurrent operator mean as:

$$\left\langle \hat{i}_{BD}^{(I)} \right\rangle = 2C_{si}\underbrace{Re\{s\}}_{s_I} = 2C_{si}s_I, \tag{21}$$

which is proportional to the in-phase component s_I of transmitted signal constellation point. In special case, for M-ary PSK $\mathrm{Re}\{s\} = \cos\phi$ that is the same as the Eq. (8).

By setting $\varphi_1 = \pi/2$ and $\varphi_2 = \pi/2$, we obtain the BD photocurrent operator mean as follows:

$$\left\langle \hat{i}_{BD}^{(Q)} \right\rangle = 2C_{si}\underbrace{Im\{s\}}_{s_Q} = 2C_{si}s_Q, \tag{22}$$

which is proportional to the quadrature component s_Q of transmitted signal constellation point. To summarize, the EA receiver form Fig. 7(a) is flexible and can be used to determine in-phase and quadrature components by properly setting the control voltages on phase trimmers, and corresponding BD photocurrent operator variance is determined as:

$$Var\left(\hat{i}_{BD}\right) = \left\langle \hat{i}_{BD}^2 \right\rangle - \left\langle \hat{i}_{BD} \right\rangle^2$$
$$= \frac{1}{4}ss^\dagger\left|e^{j\varphi_1} - e^{-j\varphi_2}\right|^2\left(2N_iN_s' + N_i + N_s' + 1 - 2C_{si}^2\right), \tag{23}$$

and it is dependent on the transmitted signal constellation point, unless $ss^\dagger = 1$. By setting $\varphi_1 = 0$ rad and $\varphi_2 = \pi$, we obtain the BD photocurrent operator variance as follows:

$$Var\left(\hat{i}_{BD}^{(I)}\right) = ss^\dagger\left(2N_iN_s' + N_i + N_s' + 1 - 2C_{si}^2\right). \tag{24}$$

By setting $\varphi_1 = \pi/2$ and $\varphi_2 = \pi/2$, BD photocurrent operator variance corresponds to that of the quadrature channel:

$$Var\left(\hat{i}_{BD}^{(Q)}\right) = ss^\dagger\left(2N_iN_s' + N_i + N_s' + 1 - 2C_{si}^2\right). \tag{25}$$

For M-ary PSK $ss^\dagger = 1$ and the variance is transmitted signal constellation point independent.

To be able simultaneously detect both in-phase and quadrature components, we need to use the 2 × 4 optical hybrid-based EA heterodyne/intradyne receiver provided in Fig. 8. The BD in the upper branch is used to detect the in-phase component, while the BD in the lower branch is

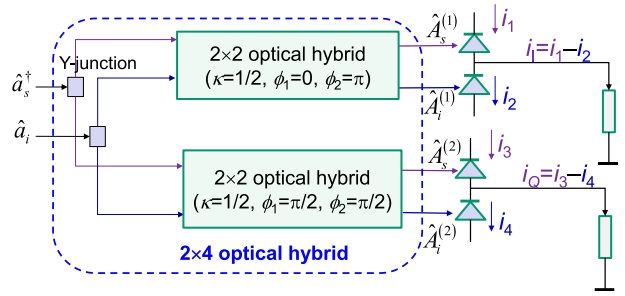

FIGURE 8. The 2 × 4 optical hybrid-based heterodyne/intradyne EA receiver suitable for demodulation of arbitrary 2-D constellation.

used to detect the quadrature component. In this EA receiver, two additional Y-junctions are required, the first for signal mode and the second for idler mode. So, we need to adjust the transmit TMSV state so that the Eqs. (21) and (22) can be used to describe photocurrents mean values corresponding to in-phase and quadrature components, while Eqs. (24) and (25) to describe the corresponding variances.

For Gaussian modulation (GM) we described above, and OH-based EA demodulator shown in Fig. 8, the corresponding channel capacity, based on Eqs. (21), (22), (24), and (25) becomes:

$$C = \log_2\left[1+\frac{\left\langle \hat{i}_{BD}^{(I)}\right\rangle^2+\left\langle \hat{i}_{BD}^{(Q)}\right\rangle^2}{Var\left(\hat{i}_{BD}^{(I)}\right)+Var\left(\hat{i}_{BD}^{(Q)}\right)}\right]$$
$$= \log_2\left(1+\frac{4TN_s\left(N_s+1\right)\left(s_I^2+s_Q^2\right)}{2ss^{\dagger}\left(2N_iN_s^{''}+N_i+N_s^{''}+1-2C_{si}^2\right)}\right)$$
$$= \log_2\left(1+\frac{4TN_s\left(N_s+1\right)}{2\left(2N_iN_s^{''}+N_i+N_s^{''}+1-2C_{si}^2\right)}\right), \quad (26)$$

where $N_s^{''}=N_sT+N_b$, and we used the fact that $ss^{\dagger}=|s|^2=s_I^2+s_Q^2$.

V. ILLUSTRATIVE RESULTS

The *Holevo capacity*, representing the quantum limit of classical capacity, is determined by [4]

$$C_{Hol}=g(TN_s+N_b)-g(N_b), \quad (27)$$

where $g(x)=(x+1)\log_2(x+1)-x\log_2 x$.

On the other hand, the *EA capacity* is given by [6]

$$C_{EA}=g\left(N_s\right)+g\left(N_s^{''}\right)-\left[g\left(\frac{\nu_+-1}{2}\right)+g\left(\frac{\nu_--1}{2}\right)\right], \quad (28)$$

where symplectic eigenvalues are defined by

$$\nu_{\mp}=\sqrt{\left(N_s+N_s^{''}+1\right)^2-4TN_s\left(N_s+1\right)}\mp\left(N_s^{''}-N_s\right). \quad (29)$$

Both quadratures of a Gaussian state cannot be simultaneously measured with the complete precision, according to the uncertainty principle. To comply, for homodyne detection we

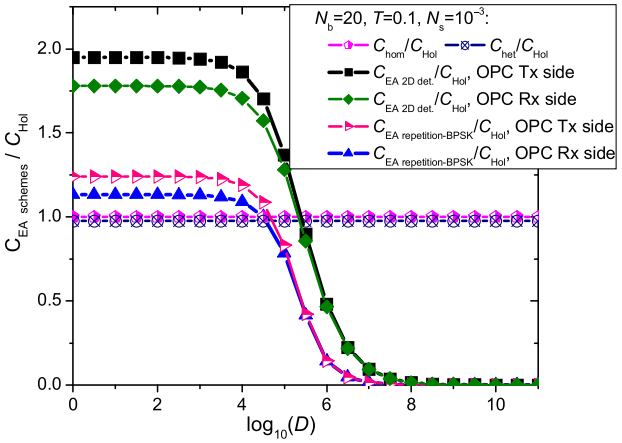

FIGURE 9. The capacity improvements of EA scheme with 2D detector and OPC on transmitter side over Holevo capacity vs. number of signal-idler modes for $N_s = 10^{-3}$, $N_b = 20$, and $T = 0.1$.

encode the information on a single quadrature so that $4TN_s$ denotes the average number of received photon, $2N_b+1$ denotes the average number of noise photons, so that the corresponding *homodyne classical capacity* is given by $C_{\text{hom}}=0.5\log_2[1+4TN_s/(2N_b+1)]$.

In heterodyne detection both quadratures can be used, without violating the uncertainty principle, so that the average number of received signal photons is given by $4TN_s\times0.5\times0.5=TN_s$ (the first 0.5 comes from splitting of quadratures and the second 0.5 originates from the heterodyne splitting), so that the average number of noise photons per quadrature is determined by $(2N_b+1)\times0.5+0.5=N_b+1$. Therefore, the *heterodyne classical channel capacity* is determined by $C_{het}=\log_2[1+TN_s/(N_b+1)]$.

Let us first evaluate the capacity improvement of the proposed EA communication scheme, with OPC on transmitter side and GM, over the Holevo capacity. For channel transmissivity $T=0.1$, average number of background photons $N_b=20$, and the average signal photon number $N_s=10^{-3}$, from Fig. 9 we conclude that this EA scheme (with GM and OPC on transmitter side) outperforms the Holevo capacity by >1.95 times for number of signal-idler Bosonic modes up to $D=94$. On the other hand, the repetition-BPSK based EA scheme (introduced in Reference [5]), but with OPC on transmitter side instead, employing receivers shown in Figs. 7 and 8, outperforms the Holevo capacity >1.2 times for number of signal-idler modes up to 6075. The EA scheme with OPC on transmitter side for up to 3000 modes outperforms the corresponding scheme with OPC on receiver side by >1.1 times. In repetition-BPSK, proposed in [5], the same BPSK signal is transmitted over all Bosonic modes, and channel capacity is calculated per single mode. (An interested reader is referred to Reference [5] for additional details.)

By close inspection of Fig. 9, contrary to Reference [5], we conclude that, when the OPC is placed on transmitter side, the large number of signal-idler modes is not really required; instead, the single signal-idler pair is enough.

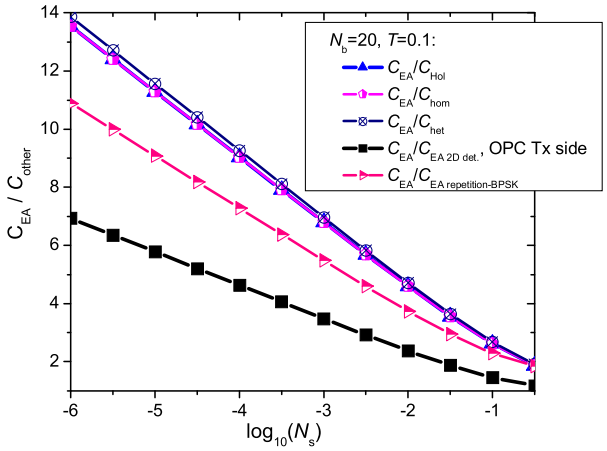

FIGURE 10. The EA capacity improvements over Holevo, homodyne, heterodyne, and proposed EA scheme (with OPC on transmitter side) against the average number of signal photons for $N_b = 20$ and $T = 0.1$.

This motivates to study how the capacity of proposed scheme with GM compares against the EA capacity and corresponding results are summarized in Fig. 10, in which the simulation parameters are selected as: channel transmissivity $T = 0.1$ and average number of background photons $N_b = 20$. Evidently, the capacity of the EA scheme, with GM and OPC on transmitter side, is significantly better compared to EA repetition-BPSK, homodyne, and heterodyne capacities.

VI. CONCLUDING REMARKS

EA communication has been proposed as an alternative to classical communication in low-brightness and highly noisy regime. The most popular EA receiver employs the OPC on receiver side. In this paper, we have proposed to place the OPC module on transmitter side instead, where signal photon has high brightness. This has allowed us to extend the transmission distance, because the low-brightness regime is now defined as $TN_s \ll 1$. Moreover, an arbitrary 2-D coherent detection scheme, developed for classical communication applications, is directly applicable in the proposed EA scheme.

The proposed EA scheme, employing the 2-D EA demodulator and transmitter side OPC, significantly outperforms EA repetition-BPSK, homodyne, heterodyne, and Holevo capacities. At the same time the EA communication scheme, in which OPC is placed on transmitter side, outperforms the corresponding scheme when OPC is used on receiver side.

REFERENCES

[1] G. Cariolaro, *Quantum Communications*. Cham, Switzerland: Springer 2015.
[2] I. B. Djordjevic, *Quantum Information Processing, Quantum Computing, and Quantum Error Correction: An Engineering Approach*, 2nd ed. San Diego, CA, USA: London, 2021.
[3] I. B. Djordjevic, *Physical-Layer Security and Quantum Key Distribution*. Cham, Switzerland: Springer, 2019.
[4] A. Holevo and R. Werner, "Evaluating capacities of bosonic Gaussian channels," *Phys. Rev. A, Gen. Phys.*, vol. 63, no. 3, Feb. 2001, Art. no. 032312.
[5] H. Shi, Z. Zhang, and Q. Zhuang, "Practical route to entanglement-assisted communication over noisy bosonic channels," *Phys. Rev. A, Gen. Phys.*, vol. 13, no. 3, Mar. 2020, Art. no. 034029.
[6] I. B. Djordjevic, "On entanglement assisted classical optical communications," *IEEE Access*, vol. 9, pp. 42604–42609, 2021.
[7] I. Djordjevic, "Quantum receivers for entanglement assisted classical optical communications," *IEEE Photon. J.*, vol. 13, no. 3, pp. 1–14, Jun. 2021.
[8] Z. Zhang and Q. Zhuang, "Distributed quantum sensing," *Quantum Sci. Technol.*, vol. 6, no. 4, Oct. 2021, Art. no. 043001.
[9] A. M. Childs, "Secure assisted quantum computation," *Quantum Info. Comput.*, vol. 5, no. 6, pp. 456–466, Sep. 2005.
[10] Q. Zhuang, Z. Zhang, and J. H. Shapiro, "Optimum mixed-state discrimination for noisy entanglement-enhanced sensing," *Phys. Rev. Lett.*, vol. 118, no. 4, Jan. 2017, Art. no. 040801.
[11] S. L. Jansen, D. V. D. Borne, P. M. Krummrich, S. Spalter, G. D. Khoe, and H. D. Waardt, "Long-haul DWDM transmission systems employing optical phase conjugation," *IEEE J. Sel. Topics Quantum Electron.*, vol. 12, no. 4, pp. 505–520, Jul. 2006.
[12] Z.-Y. J. Ou, *Quantum Optics for Experimentalists*. Singapore: World Scientific, 2017.
[13] I. B. Djordjevic, *Advanced Optical and Wireless Communications Systems*. Cham, Switzerland: Springer, 2018.

IVAN B. DJORDJEVIC (Fellow, IEEE) received the Ph.D. degree from the University of Nis, Yugoslavia, in 1999.

He is currently a Professor of electrical and computer engineering and optical sciences with the University of Arizona. He is also the Director of the Optical Communications Systems Laboratory (OCSL) and the Quantum Communications (QuCom) Laboratory and the Co-Director of the Signal Processing and Coding Laboratory. Prior to joining the University of Arizona, he held appointments at the University of Bristol, U.K.; the University of the West of England, U.K.; Tyco Telecommunications, USA; the National Technical University of Athens, Greece; and State Telecommunication Company, Yugoslavia. He has authored or coauthored eight books, more than 550 journals and conference publications, and holds 54 US patents.

Dr. Djordjevic is the OSA (Optica) Fellow. He serves as an Area Editor/Associate Editor/member of Editorial Board for IEEE TRANSACTIONS ON COMMUNICATIONS, OSA (Optica)/IEEE JOURNAL OF OPTICAL COMMUNICATIONS AND NETWORKING, *Optical and Quantum Electronics*, and *Frequenz*. He was serving as an Editor/Senior Editor/Area Editor for IEEE COMMUNICATIONS LETTERS, from 2012 to 2021. He was serving as an Editorial Board Member/Associate Editor for *Journal of Optics* (IOP) and *Physical Communication* journal (Elsevier), from 2016 to 2021.